Probability distribution functions and coherent structures in a turbulent channel

E. Lamballais,[1,2] M. Lesieur,[1,*] and O. Métais[1]
[1]*LEGI Institut de Mécanique de Grenoble, Institut National Polytechnique de Grenoble, Université Joseph Fourier and Centre National de la Recherche Scientifique, Boîte Postale 53, 38041 Grenoble Cedex 9, France*
[2]*Laboratoire d'Etudes Aérodynamiques, UMR 6609, Centre d'Etudes Aérodynamiques et Thermiques, 43 route de l'Aérodrome, 86036 Poitiers Cedex, France*
(Received 21 April 1997; revised manuscript received 4 August 1997)

With the aid of a direct numerical simulation of an incompressible plane turbulent channel at $h^+=162$, we have determined the probability distribution functions (PDF's) of pressure and of the various velocity components from the wall to the channel center. The pressure turns out to be symmetric with exponential tails at the wall as well as at $y^+=2.5$. At $y^+=12$, where the streamwise streaks intensity is maximum, the pressure has become asymmetric. This character intensifies with the distance away from the wall and the distribution obtained in the channel center resembles those determined in isotropic turbulence and free-shear flows. Very close to the wall ($y^+=2.5$), the PDF of u' is highly skewed, with exponential and sub-Gaussian distributions at high and low values, respectively. This indicates that the high-speed streaks are very intermittent at the wall. The reverse occurs close to the channel center, where intense negative u' prevail. Then we show that the most probable orientation of the fluctuating vorticity vector is perpendicular to the wall in the region $5<y^+<30$ (which is basically in the low- and high-speed regions), while it is 45° with respect to the wall above. [S1063-651X(97)06712-3]

PACS number(s): 47.27.−i

I. STREAMWISE STREAKS IN TURBULENT BOUNDARY LAYERS

It is well established since the experiments of Kline *et al.* [1] in the turbulent boundary layer that streamwise streaks of low and high longitudinal velocity (with respect to the local mean velocity profile) exist close to the wall, between approximately (in wall units ν/v_*) $y^+=5$ and $y^+=40$–50. The same low- and high-speed streaks were found in the turbulent channel since the large-eddy simulations of [2] [see also the direct numerical simulation (DNS) of [3]].

We study here a fluid of uniform density between two infinite parallel flat plates. Let x,y,z be the longitudinal, transverse, and spanwise directions, respectively. We solve numerically the unstationary Navier-Stokes equations, with periodic boundary conditions in the streamwise and spanwise directions, and adherence at the walls. We use a mixed numerical method: desaliased pseudospectral along (x,z) and finite differences of order six (compact schemes) along y. These schemes reach a quasispectral precision, while allowing more flexibility in the choice of the computational grid. Temporal integration uses Crank-Nicholson and third-order Runge-Kutta schemes for the viscous and nonlinear terms, respectively. The incompressibility condition is ensured up to the zero machine in all the computation domain and at each time step by a fractional steps method. We define the macroscopic Reynolds number $\mathrm{Re}=U_m 2h/\nu$ based upon the bulk velocity U_m and the width of the channel $2h$. The width of the calculation domain is $(L_x,L_y,L_z)=(4\pi h,2h,2\pi h)$, which requires 128×128 Fourier (dealiased) modes in (x,z) directions and 129 grid points along y. The initial condition corresponds to a field computed from a large-eddy simulation using a subgrid-model based upon a spectral eddy-viscosity corrected to account for the deviation of the kinetic-energy spectra from a Kolmogorov one [4]. Calculations have been done at constant U_m and pursued up to complete statistical stationarity. The Reynolds number is $\mathrm{Re}=5000$, corresponding for the developed turbulence regime to a friction Reynolds number $h^+=v_* h/\nu=162$. This Reynolds number is subcritical from the point of view of linear-stability theory, as in the DNS of Kim *et al.* [3] done at $\mathrm{Re}_m=5600$, where the main characteristics of a turbulent channel flow was observed. The grid is refined close to the wall, with a first point at $y^+=1$. Statistics are obtained by temporal averaging, as well as averaging in the directions x,z. Consideration of both sides of the channel allows us to double the number of statistical samples.

Numerical simulations have confirmed the experimental findings that vorticity patches located just above the low-speed streaks may be ejected away from the wall. This produces hairpin vortices apparently stretched by the ambient shear. It is by this ejection mechanism that vorticity at the wall is transported into the boundary layer, making it turbulent.

There is still much controversy about the interpretation of the streamwise streaks and how they relate to the ejection of hairpins. However, most people agree on the points that low-speed streaks correspond to fluid rising away from the wall with, as a result, production of a locally inflectional longitudinal velocity profile, above which one might explain the vorticity ejections through local Kelvin-Helmholtz instabilities. High-speed streaks are, on the contrary, regions of descending flow sweeping to the wall. Here the local longitudinal velocity profiles are not inflectional and sweeps produce instantaneous local spanwise vorticities at the wall two or three times higher (in modulus) than the average value at the wall v_*^2/ν (see [5]). It is thus under the high-

*Electronic address: Marcel.Lesieur@hmg.inpg.fr

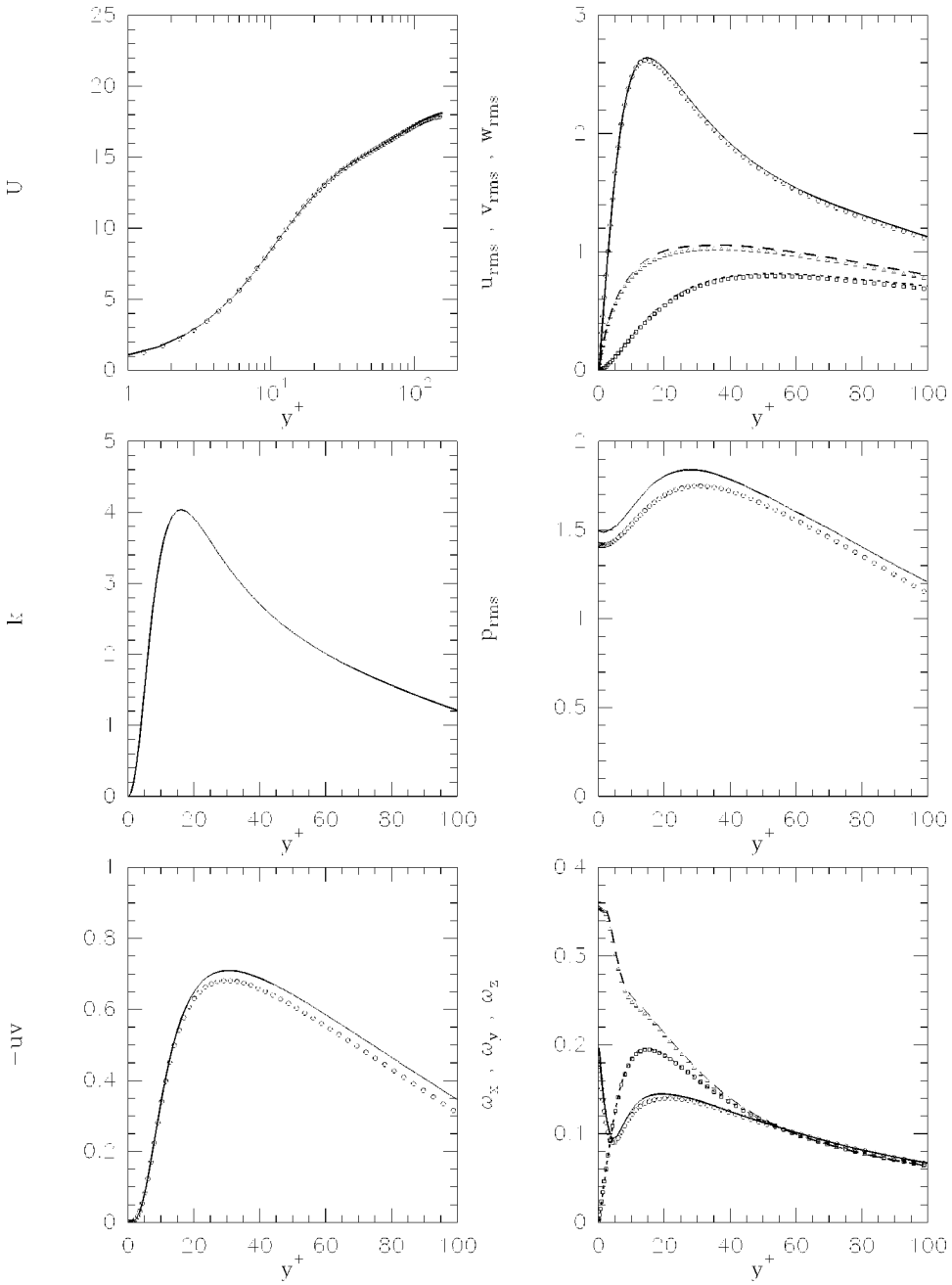

FIG. 1. Statistical data obtained in the DNS of a turbulent channel flow from present simulations (straight line) and Kuroda [6] (symbols): (a) mean velocity, (b) rms velocity fluctuations (respectively from top to bottom, longitudinal, spanwise, and vertical), (c) kinetic energy, (d) rms pressure fluctuation, (e) Reynolds stresses, and (f) rms vorticity (from top to bottom, spanwise, vertical, and longitudinal).

speed streaks that most of the drag is produced at the wall.

In Fig. 1 the present statistics (the DNS at $h^+=162$) are compared with a previous DNS carried out in [6] using spectral methods at $h^+=150$. These DNS's, which use precise numerical methods, turn out to be in good agreement with the experiments [7]. We see in Fig. 1(a) that the logarithmic range on mean velocity profile begins at $y^+=30$. We show in Fig. 1(b) the rms velocity-fluctuation profiles as a function of y^+. The u' peak at $y^+=12$ corresponds to the maximal intensity of the streamwise velocity streaks. The transverse velocity v' is lower than w' everywhere. This can be easily explained close to the wall when considering the continuity equation, which implies $w' \propto y^+$ and $v' \propto (y^+)^2$. Figure 1(e) shows the Reynolds stresses, whose peak is higher (at the bottom of the logarithmic layer), which is the signature of ejections of vorticity from the wall. The same peak is observed for the pressure fluctuations [Fig. 1(d)], which is certainly due to the low pressure associated with the high vorticity at the tip of the ejected hairpin. Finally Fig. 1(f) shows the rms vorticity fluctuations, a quantity very difficult to measure precisely experimentally. It indicates that the maximum vorticity produced is spanwise and at the wall, in fact under the high-speed streaks, as discussed above. The rms vorticity perpendicular to the wall is about 30% higher than

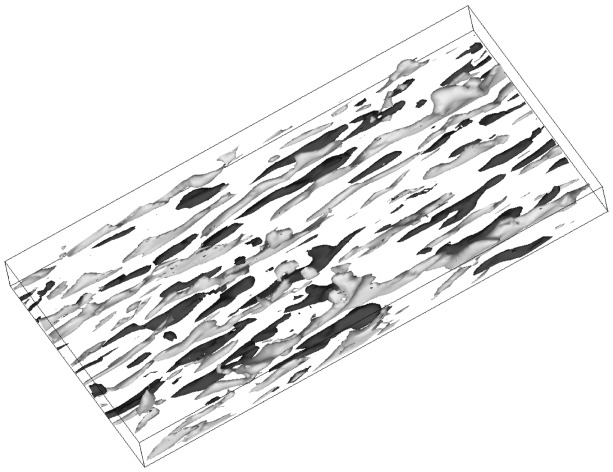

FIG. 2. Low- and high-speed streamwise streaks, visualized by contours of positive (dark) and negative (gray) longitudinal velocity fluctuations ($u'^+ = \pm 3.3$) in the DNS of a turbulent channel close to one wall ($h^+ = 162$).

the longitudinal vorticity in the region $5 < y^+ < 30$. This is another statistical indicator of the streaks. In Fig. 2 we present isosurfaces of positive and negative fluctuating longitudinal velocities ($u'^+ = \pm 3.3$). This instantaneous visualization shows clearly the streaks' organization near the wall and their coherence in the streamwise direction.

II. PROBABILITY DISTRIBUTION FUNCTIONS OF PRESSURE AND VELOCITY

In a turbulent flow, coherent vortices are generally characterized by a high-vorticity modulus and a low pressure. It was shown in [8] that the pressure probability distribution function (PDF) was skewed in isotropic turbulence, with an exponential tail in the low-pressure regions and a Gaussian tail in the high-pressure regions. On the other hand, the PDF of any vorticity component is symmetric, with exponential-like tails. Analogous results were found in the DNS of a mixing layer [9] and, for the pressure, in experiments of turbulence between two counterrotating disks [10] and in a jet [11]. In all these cases, the coherent vortices are clearly identified. It is thus of interest to carry out the same study in a plane turbulent channel in order to see how the various PDF's of pressure and velocity react to the existence of streaks and ejected hairpins. All the PDF's presented now concern the fluctuations with respect to the mean, and the argument is normalized by the rms value. They are plotted in semilogarithmic coordinates and the dashed parabola indicates a Gaussian distribution of variance 1.

Figure 3 shows the PDF's of pressure at the wall, very close to the wall in the viscous region ($y^+ = 2.5$), where the streaks are maximum ($y^+ = 12$), and in the core of the flow at the channel center ($y^+ = 162$). Figures 4, 5, and 6 present, respectively, the longitudinal (u'), transverse (v'), and spanwise (w') velocity fluctuations at $y^+ = 2.5$, 12, and 162. The pressure PDF at the wall ($y^+ = 0$) is symmetric, with exponential wings. There is no trace of any kind of vortical organization on it. Note that such a pressure PDF had already

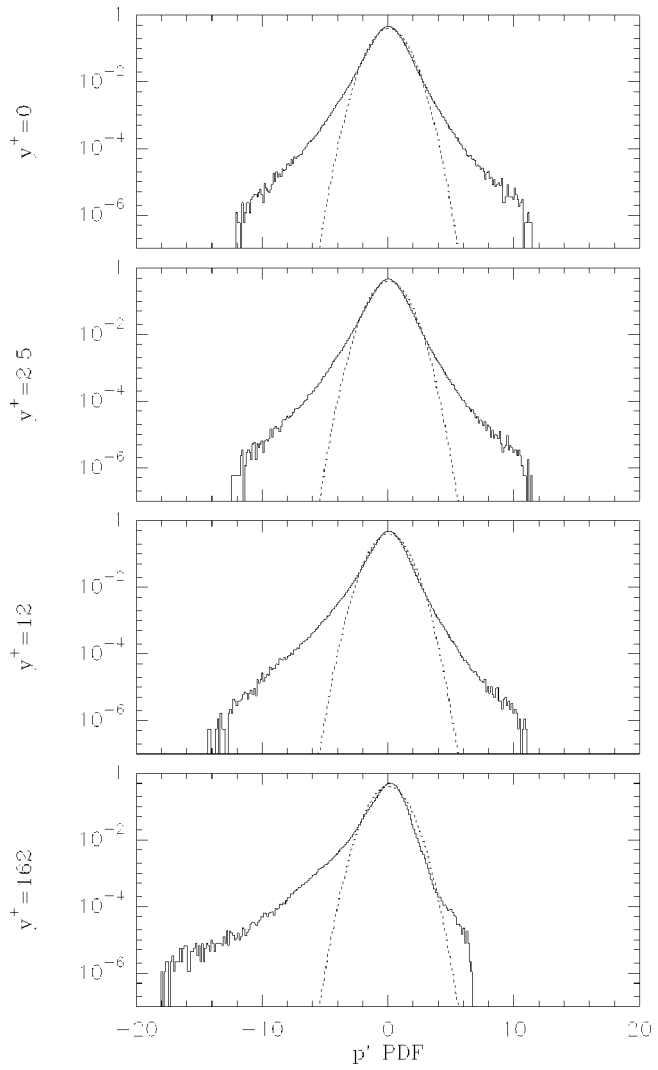

FIG. 3. Probability density distibution of the pressure fluctuations for different y locations.

been determined in analogous simulations by Kim [12], but not in logarithmic coordinates, and with a smaller number of statistical samples. Note that the wall measurements in the laboratory experiment of the flow between counterrotating disks performed by Cadot *et al.* [13] show asymmetric distributions. The apparent imcompatibility with the present observation comes from the very distinct generation mechanism of the flow vortices. As stressed above, the hairpin vortices of the channel flow are not created in the immediate vicinity of the wall and no vortex seems to be present in this region of the flow. In the experiment by Cadot *et al.* [13], the two counterrotating disks generate a high-shear region in the middle of the tank, which leads to intense vortices resulting from Kelvin-Helmholtz instability. The latter, in their further evolution, eventually impact the wall, yielding very intermittent low-pressure peaks and asymmetric pressure signals. Turning back to our channel DNS, at $y^+ = 2.5$, the pressure is very close to the distribution at the wall and it is still difficult to see on it any trace of vortices. The longitudinal velocity is highly intermittent in the high speeds and ''sub-Gaussian'' in the low speeds. Thus high-speed streaks are

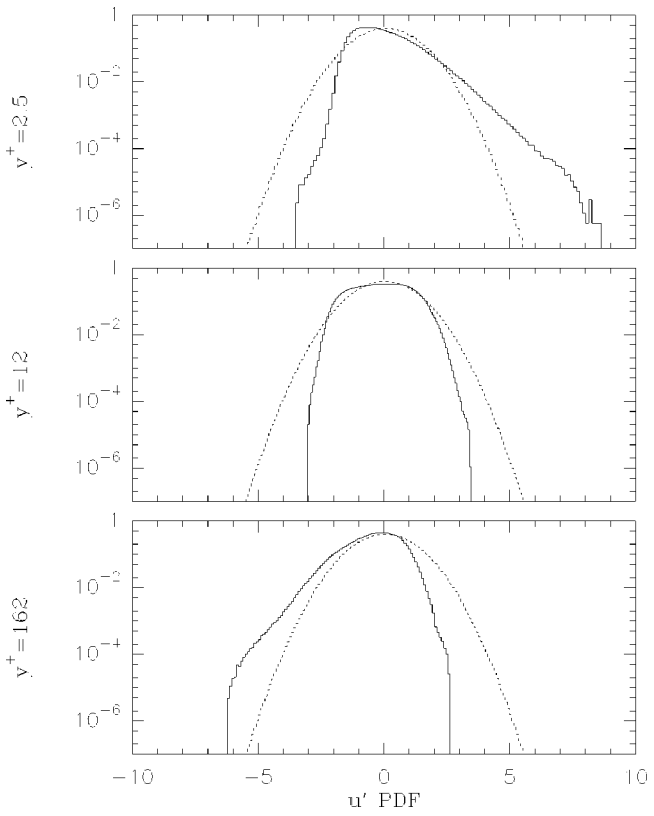

FIG. 4. Probability density distibution of the longitudinal velocity fluctuations for different y locations.

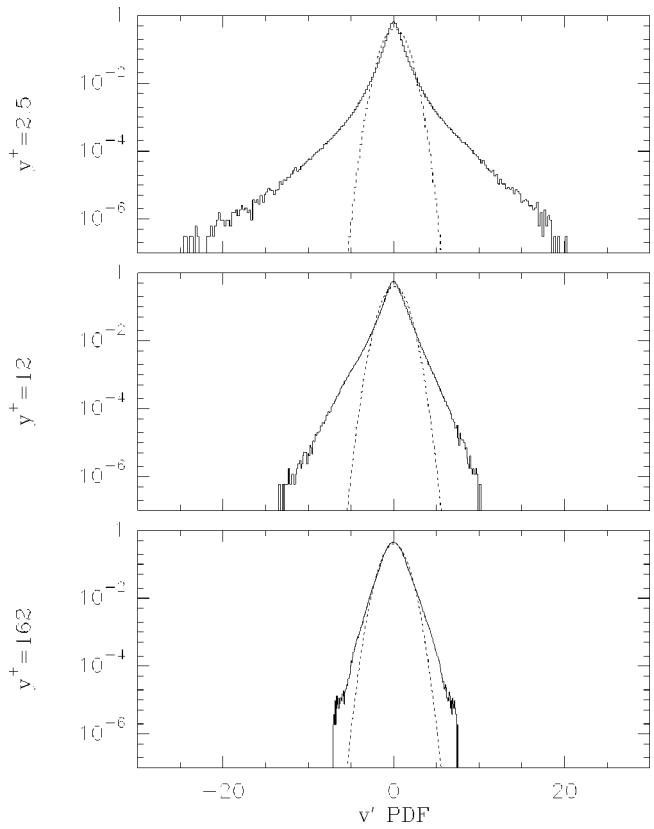

FIG. 5. Probability density distibution of the transverse velocity fluctuations for different y locations.

much more intense and intermittent than the low-speed ones close to the wall. Such a distribution for u' at the wall is responsible for the positive skewness measured in the experiments of [14] and recovered in the DNS of [12]. Another consequence of these abrupt excursions of longitudinal velocity in the high-speed streaks close to the wall is the creation of intense fluctuations of spanwise vorticity (and hence of drag) at the wall just underneath and of same sign as the basic vorticity. This was noticed by Ducros *et al.* [5] in large-eddy simulations of a weakly compressible boundary layer spatially developing above a flat plate. Still at $y^+=2.5$, the PDF of v' is very intermittent, with faster descents than ascents. This is in agreement with the fact that the flow is upward in the low-speed regions and downward in the high-speed regions. As for the spanwise velocity w', the flow is extremely intermittent. It should be symmetric, due to the mirror symmetry of turbulence with respect to planes parallel to (x,y). The slight asymmetry is certainly attributable to the length of the statistical sampling, insufficient for the larger vortices that travel within the channel.

In the core of the streaks ($y^+=12$), u' has no intermittency at all since both sides of the PDF are sub-Gaussian. It seems to indicate that the streaks are, at this level, weakly random components of the flow. The distribution of v' is weakly asymmetric, with still a preference more in favor of the descents than the ascents. w' is not very intermittent. The pressure becomes asymmetric with more intermittency in the troughs than in the high pressure regions, which are still exponential. In the central region of the channel ($y^+=162$), the pressure PDF resembles skewed distributions encoun-

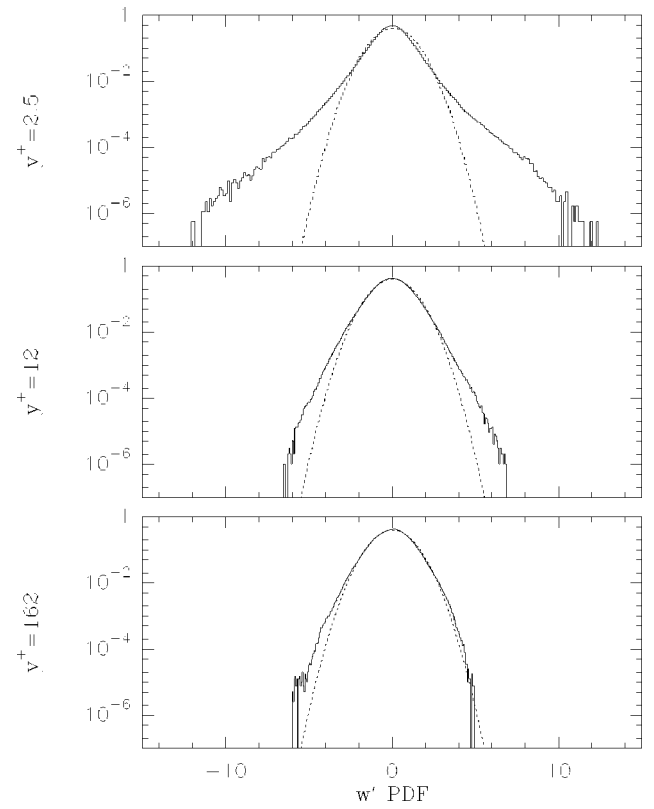

FIG. 6. Probability density distibution of the spanwise velocity fluctuations for different y locations.

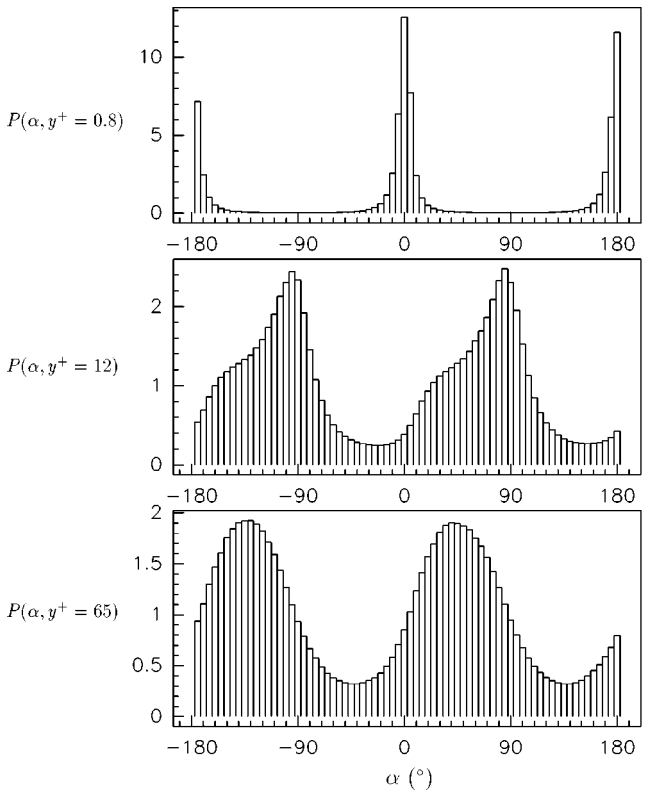

FIG. 7. PDF of the inclination angle α at three y locations.

tered in isotropic turbulence or free-shear flows. Visualizations of the vorticity field show in fact that large Λ-shaped vortices are carried by the flow, and their existence might explain the pressure distribution. v' and w' look like isotropic turbulence. As for u', it is now preferably negative, with excursions of low speeds. It seems then that the intermittent sweeps of high speed at the wall are balanced by low speeds in the channel center, which is quite natural if one thinks in terms of continuity.

III. PREFERRED INCLINATION OF THE VORTICITY

We consider the PDF of $\alpha = \arctan(\omega_y/\omega_x)$, the angle made with the wall by the vorticity vector projected in the (x,y) plane. Such PDF's have already been determined in the large-eddy simulation of a turbulent channel flow [15]. Away from the wall ($0.2 < y/h < 0.8$), the most probable value of α was found to be close to 45°, indicating a tendency for the hairpin vortices to be aligned with the first principal axis of the mean deformation tensor. This reference does not provide information on the PDF of α in the range $5 < y^+ < 30$. The PDF $P(\alpha, y^+)$ is shown in Fig. 7. Each contribution is weighted by the magnitude of the projected vorticity to give a greater impact of high-vorticity regions on the statistics. Figure 7 displays this distribution for three y positions. Very close to the wall [Fig. 7(a)], α tends to be zero, reflecting simply the boundary condition $\omega_y = \partial u/\partial z - \partial w/\partial x = 0$ at the wall (where u and w are zero). Further from the wall ($y^+ = 12$), in the streaks region, $P(\alpha, y^+)$ is skewed with a sharp peak near 90° [Fig. 7(b)]. Finally, the preferential inclination at 45° is recovered in the outer region [Fig. 7(c)]. We have checked that non-weighted PDF's of α exhibit similar behavior, except that the peaks $P(\alpha, y^+)$ are then less strongly marked. In fact, a distribution of the type in Fig. 7(b) with a peak at 90° is recovered from $y^+ = 5$ to $y^+ = 30$, as shown in [16].

We see in Fig. 1 that at $y^+ = 65$, the rms of vorticity components are close (isotropy tendency). A rough evaluation of the mean orientation angle $\langle \alpha \rangle \approx \arctan(\omega_y^{rms}/\omega_x^{rms})$ yields 45°, in good agreement with the mean value obtained from the symmetric PDF at this level. On the other hand, we have $\omega_y^{rms} \approx 1.5 \omega_x^{rms}$ at $y^+ = 12$, which would yield $\langle \alpha \rangle \approx 56°$ with the same approximate reasoning. It is clear that this value is close to the mean value of the corresponding skewed PDF.

These results indicate that the vorticity vector tends to rise (with respect to the x-z plane) in the streaks region. This is not in favor of the existence of longitudinal vortices stretched by the flow in this region, often invoked in order to explain the streaks [17,18].

IV. CONCLUSION

On the basis of an accurate direct numerical simulation of a turbulent plane channel at $h^+ = 162$, we have determined the PDF's of the pressure at the wall and of the pressure and velocity fluctuations at $y^+ = 2.5$, 12, and 162. The pressure at the wall is symmetric with exponential tails and seems not to be affected by the existence of coherent vortices, nor by the high and low-speed streaks system. The pressure at $y^+ = 2.5$ is very similar to the pressure at the wall, while the velocity fluctuations show very intermittent rapidly descending high-speed streaks and more smoothly ascending low-speed streaks. At $y^+ = 12$, the streaks system is weakly random with sub-Gaussian PDF's for u'. The pressure PDF has become asymmetric. At $y^+ = 162$, the pressure has an exponential tail in the low-pressure regions and is close to Gaussian in the high-pressure regions. This looks very much like the pressure PDF's observed in isotropic turbulence or free-shear flow and is generally associated with the presence of coherent vortices. In the channel, the coherent vortices are hairpin and Λ vortices of various sizes ejected from the wall. In the channel center, the PDF of u' shows now the predominance of intense low-speed fluctuations.

We have also looked at the PDF of α, the inclination angle of the fluctuating vorticity vector with respect to the wall, in the same way as Moin and Kim [15] with the aid of large-eddy simulations. They considered the range $y^+ > 30$ and found that the PDF of α peaks at 45°. We have indeed recovered this result. However, we have also found in the range $5 < y^+ < 30$ a peak in the PDF at 90°. These results might question the hypothesis that longitudinal vortices exist close to the wall, often made by various authors [17,18] in order to explain the streaks.

ACKNOWLEDGMENTS

We wish to thank Emmanuel Villermaux for stimulating discussions. Computations were carried out at the Institut du Développement et des Ressources en Informatique Scientifique (IDRIS), Paris.

[1] S. J. Kline, W. C. Reynolds, F. A. Schraub, and P. W. Runstadler, J. Fluid Mech. **95**, 741 (1967).
[2] P. Moin and J. Kim, J. Fluid Mech. **118**, 341 (1982).
[3] J. Kim, P. Moin, and R. Moser, J. Fluid Mech. **177**, 133 (1987).
[4] E. Lamballais, O. Métais, and M. Lesieu, in *Direct and Large Eddy Simulation II*, edited by J. P. Chollet, P. R. Voke, and L. Kleiser (Kluwer Academic, Dordrecht, 1997), p. 225.
[5] F. Ducros, P. Comte, and M. Lesieur, J. Fluid Mech. **326**, 1 (1996).
[6] A. Kuroda, Ph.D. thesis, University of Tokyo, 1990 (unpublished).
[7] F. Durst, H. Kikura, I. Lekakis, J. Jovanić, and Q. Ye, Exp. Fluids **20**, 417 (1996).
[8] O. Métais and M. Lesieur, J. Fluid Mech. **239**, 157 (1992).
[9] P. Comte, M. Lesieur, and E. Lamballais, Phys. Fluids A **4**, 2761 (1992).
[10] S. Fauve, C. Laroche, and B. Castaing, J. Phys. II **3**, 271 (1993).
[11] Y. Gagne (private communication).
[12] J. Kim, J. Fluid Mech. **205**, 421 (1989).
[13] O. Cadot, D. Douady, and Y. Couder, Phys. Fluids **7**, 630 (1995).
[14] G. Comte-Bellot, Ph.D. thesis, University of Grenoble, 1963.
[15] P. Moin and J. Kim, J. Fluid Mech. **155**, 441 (1985).
[16] E. Lamballais, Ph.D. thesis, Institut National Polytechnique de Grenoble, 1996 (unpublished).
[17] S. K. Robinson, Annu. Rev. Fluid Mech. **23**, 601 (1991).
[18] J. M. Hamilton, J. Kim, and F. Waleffe, J. Fluid Mech. **287**, 317 (1995).